

Photoemission and band-structure results for NiSi₂

Y. J. Chabal, D. R. Hamann, J. E. Rowe, and M. Schlüter

Bell Laboratories, Murray Hill, New Jersey 07974

(Received 8 December 1981)

Photoemission measurements on bulk NiSi₂ are interpreted on the basis of linear augmented-plane-wave band-structure calculations. The emerging picture describes NiSi₂ as a "noble-metal" compound, consisting of a metallic, simple cubic silicon crystal which is stabilized by Ni anions.

I. INTRODUCTION

Silicon and transition metals can form a variety of stable compounds. While many aspects of the compound formation have been investigated,¹⁻⁴ a general understanding is still lacking. Of particular interest is also the formation of silicide-Si contacts⁵⁻⁹ which play an important technological role as rectifying Schottky-barrier devices. There is thus need to study and characterize both silicide bulk phases and interfaces.

As part of an ongoing investigation we report here theoretical band-structure results and angle-integrated ultraviolet photoemission (UPS) measurements of one particular silicide, NiSi₂. This particular compound displays perfect epitaxial growth on Si(111) surfaces, with an atomically abrupt interface.¹⁰ Thus Si-NiSi₂ is an ideal system in which to explore details of interface bonding.

II. PHOTOEMISSION RESULTS

Ni films (100–400 Å) were deposited by electron-gun evaporation on polished and clean Si(111) wafers at a pressure of 10⁻⁷ Torr. The samples were preannealed at 300°C for 30 min and then annealed at 800°C for 30 min at a pressure $\leq 1 \times 10^{-7}$ Torr.¹⁰ The preannealing produced polycrystalline Ni₂Si and the annealing at the elevated temperatures produced the epitaxial NiSi₂.

The crystallinity was checked by means of Rutherford backscattering and channeling. The channeled backscattering yields ($\chi \sim 5\%$ to 10%) were close to single-crystal values. The bulklike periodicity of these NiSi₂ films was shown to be well defined as was the long-range order parallel to the surface.¹¹

The samples were then introduced into the

Ultrahigh vacuum (UHV) chamber for low-energy electron diffraction (LEED), Auger, and UPS studies. The thin oxide and carbon contaminations were removed by sputtering with 500-eV Ar⁺ ions for several minutes until Auger spectroscopy showed less than 1% of a monolayer of C or O. Crystalline order and NiSi₂ stoichiometry were restored by ~ 5 -min annealing at 700°C as shown by LEED and Auger spectroscopy.¹² The samples were then ready for surface investigations. The effect of sputtering and annealing in UHV regarding the crystalline order was checked after the UHV run by Rutherford backscattering and channeling. The channeled backscattering yields were slightly lower or similar to those obtained before the UHV treatment, indicating an improvement of long-range crystallinity.

The LEED patterns obtained for electron energies between 25 and 200 eV showed an unreconstructed surface with a moderately low uniform background. The angular width of the LEED beams indicated that, if domains were present on the surface, their minimum size was 100 Å.

The photoemission spectra were obtained at 11.7, 16.8, and 21.2 eV by introducing Ar, Ne, or He in a resonance lamp. The photons were incident at 70° measured from the sample normal. The analyzer was a grid analyzer with a typical resolution of 0.3 eV. The results are shown in Fig. 1. The main feature is located ~ 3.1 eV below the Fermi energy. Weak features are also visible at 5.0, 5.8, and 1.3 eV below E_f .

III. THEORETICAL RESULTS AND DISCUSSION

The electronic structure calculations were done using a recently developed self-consistent linear augmented-plane-wave (LAPW) band-structure pro-

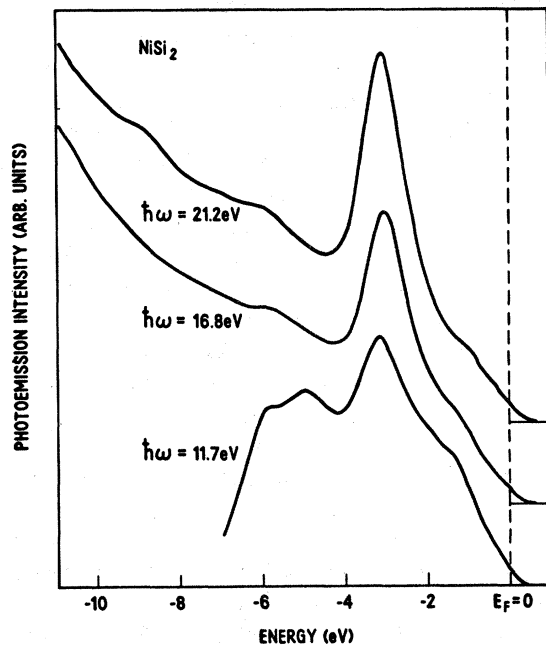


FIG. 1. Photoemission spectra of NiSi_2 for three different photon energies (21.2, 16.8, and 11.7 eV). The vertical scale is linear and the energy scale is referenced to the Fermi energy.

gram.¹³ Wave functions are represented by plane waves in interstitial regions smoothly jointed to a pair of numerical radial functions for each angular momentum component l inside touching muffin-tin spheres. The charge and potential are of completely general form, and are represented by numerical radial functions for each symmetry-allowed angular momentum component inside the muffin-tins and plane waves in the interstitial region. The Wigner interpolation formula¹⁴ is used for the local exchange and correlation potential. The total charge density is evaluated in real space, then inserted into the exchange and correlation functional which in turn is analysed in terms of Fourier and spherical harmonic expansions.

Overall 0.1-eV convergence was obtained using approximately 100 plane waves and a $l \leq 5$ expansion for the wave function, 869 plane waves and $l \leq 6$ for the charge and potential, and six special points¹⁵ for the Brillouin-zone sampling. Density-of-states spectra were evaluated from 70 k points in $\frac{1}{48}$ of the Brillouin zone.

NiSi_2 crystallizes in the calcium fluoride structure. In this structure the silicon atoms can be viewed as forming a simple cubic lattice with Ni atoms occupying the center of every other cube.

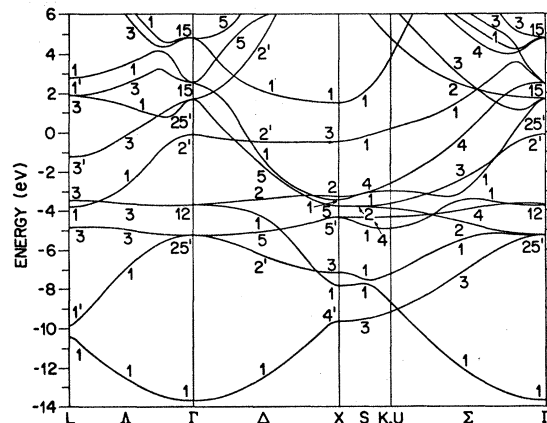


FIG. 2. Self-consistent LAPW band structure of NiSi_2 plotted along high-symmetry lines in the fcc Brillouin zone.

The lattice constant of the fcc primitive unit cell is 5.40 Å.¹⁶ Each silicon is tetrahedrally surrounded by four Ni atoms at a distance of 2.34 Å, six second-nearest Si atoms at 2.70 Å, and eight third-nearest Si atoms at 3.82 Å. Each Ni is surrounded by eight Si atoms at 2.34 Å and twelve second-nearest Ni atoms at 3.82 Å. The Si-Ni distance is nearly equal to the Si-Si distance of 2.35 Å in bulk Si.

The calculated energy bands are shown in Fig. 2 as they are plotted along various high-symmetry lines in the fcc Brillouin zone. The band structure may be viewed roughly as resulting from a superposition of a simple cubic Si lattice with about a 15-eV valence-band width and from nearly isolated, eightfold coordinated Ni atoms. The cubic crystal-field splitting of the Ni d states centered around -4 eV is about 1.7 eV ($\Gamma_{25'} - \Gamma_{12}$) and the dispersion is generally small ($\lesssim 1.0$ eV). There is, however, some Ni-Si hybridization resulting in some directional covalent bonding. This is quantitatively supported by the finite Ni d character ($\sim 40\%$ inside the Ni muffin tin) for the empty $\Gamma_{25'}$ antibonding level at ~ 1.6 eV. These antibonding wave functions contain one extra node between nearest neighbors and therefore allow admixture of Ni $4d$ character. Overall, the Ni $3d$ bands are found well below the Fermi energy suggesting an approximate "noble-metal" configuration. This point of view is clarified in Fig. 3 where we display calculated density-of-states curves. The total valence density of states (bottom panel) is decomposed into Si (top panel) and Ni (middle panel) partial densities which are fractionally

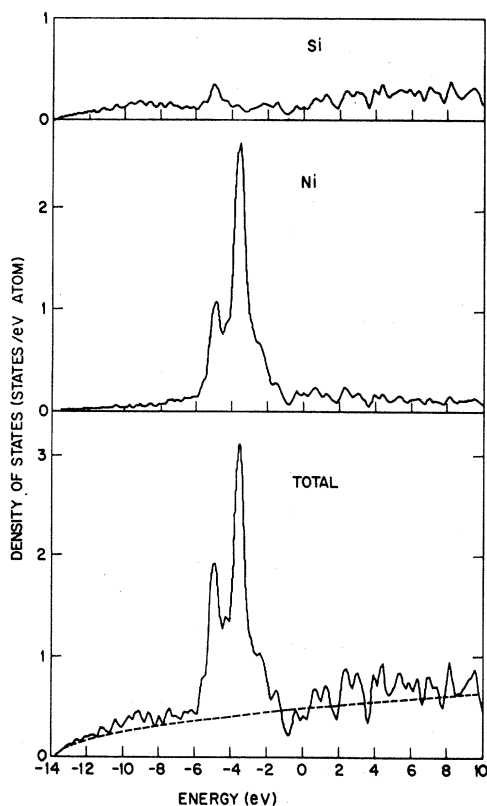


FIG. 3. Calculated density-of-states spectra for NiSi_2 . The total density (bottom) is decomposed into Ni (middle) and Si (top) contributions according to the charge integral within the muffin-tin spheres.

weighted by the charge distributions in the respective muffin-tin spheres. The silicon density of states is rather featureless and free-electron like. The weak structure around -5 eV arises mainly from Si p states. The large Ni density of states is located clearly below the Fermi level resembling more the spectrum of metallic copper than metallic nickel.¹⁷ The structures in the calculated density-of-states spectra agree well with the photoemission data in Fig. 1. The main feature observed at -3.1 eV corresponds to the (nonbonding) e_g -symmetry manifold of Ni d states, calculated at -3.5 eV. The t_{2g} manifold is more spread out by forming weakly bonding combinations with silicon s and p states. The main peak is calculated to be at -5.0 eV. The states can be identified with the structures observed between -5.0 and -5.8 eV. The variations of these features with photon energy are probably due to matrix element effects such as in the case of the Cu(111) surface.¹⁸ Therefore no conclusive information can be extracted experimen-

tally as to the relative contribution of Si or Ni to the density of states. The weak shoulder observed at -1.3 eV is due to the onset of the Ni d states. A qualitatively similar picture of Ni d states extending from about -1 to -6 eV has also been predicted recently by Bisi and Calandra¹⁹ based on empirical extended Hückel calculations. In detail, however, their density-of-states structures deviate from our LAPW results. In particular the free-electron-like background (emphasized by the dashed curve in Fig. 3) is not reproduced by the Hückel calculations. This background which is the dominant contribution at the Fermi level, results mainly from Si and Ni s and p electrons.

The key result of our analysis thus is that the metallic character of NiSi_2 does not predominantly result from Ni d electrons as in metallic Ni but rather from s - and p -like free electrons. We have, in effect, a compound noble metal. This suggests that NiSi_2 may be viewed roughly as a metallic, simple cubic Si phase²⁰ which is stabilized by the Ni atoms centered in every other cube. The mechanism of this stabilization can be understood by examining the charge-density contour plots illustrating the bonding rearrangement of charge in Figs. 4 and 5. The contours show the self-consistent crystalline charge density (Fig. 4) and a superposition of neutral atomic charge densities (Fig. 5). The plots are shown in a (110) plane extending over two Si cubes. The Ni atom at the corner (0,0) sits in the center of one Si cube while the empty center of the other Si cube is at (0.5,1). Comparison of Figs. 4 and 5 shows mainly charge accumulation along the nearest-neighbor Ni-Si directions and some small enhancement between nearest-neighbor Si atoms, while the empty cube becomes charge deficient. The figures also show the absence of any significant charge accumulation between neighboring Ni atoms. The charge contours contain the Ni d charge-density peak of Fig. 3, and their nearly spherical shape demonstrates the absence of strong directional d charge lobes (which are permitted by symmetry). This further supports the noble-metal character of Ni in NiSi_2 .

If the charge distribution around Si is compared with that of bulk Si,¹³ a remarkable similarity appears. Within a sphere drawn around the Si at its covalent radius, the buildup of charge in the tetrahedral bonding directions and its depletion in the antibonding regions is nearly identical for the two materials. The NiSi_2 charge is essentially equal to the Si charge scaled down by approximately 10%. Thus the Si can achieve its preferred

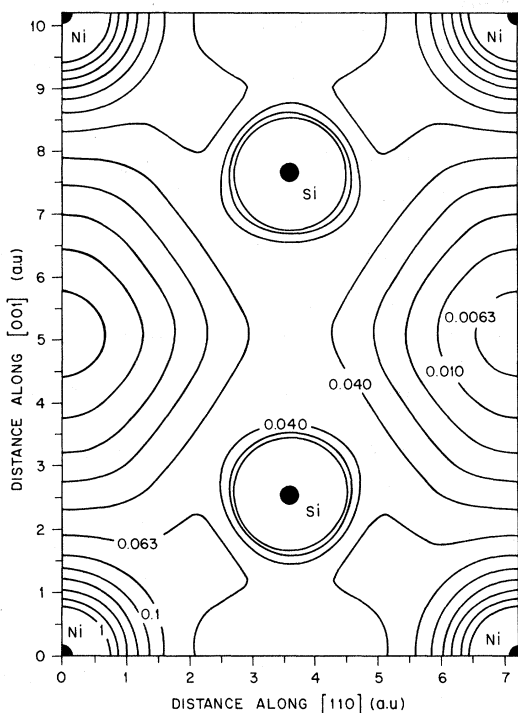


FIG. 4. Self-consistent crystalline charge density for NiSi_2 plotted in a (110) plane. The contours are given in units of electrons per cubic Bohr. Contours are logarithmically spaced, five to the decade (0.1, 0.16, 0.25, 0.40, 0.63, 1.0).

bonding configuration with only indirect Si-Si interactions through the intervening Ni. The ability of NiSi_2 to form sharp and defect-free interfaces with Si (Refs. 10 and 11) is undoubtedly aided by the fact that the charge distribution around an interface Si is nearly independent of the identity of its near neighbors.

The similarity of the Si charge distributions in NiSi_2 and bulk Si requires us to consider why the spectra are different. The answer clearly lies in the bonding topology. In Si, sp^3 hybrids face each other in pairs, and the energy splitting between the bonding and antibonding combinations is the fundamental mechanism which gives rise to the valence-conduction band gap. In NiSi_2 eight sp^3 hybrids overlap through a single Ni, and the sim-

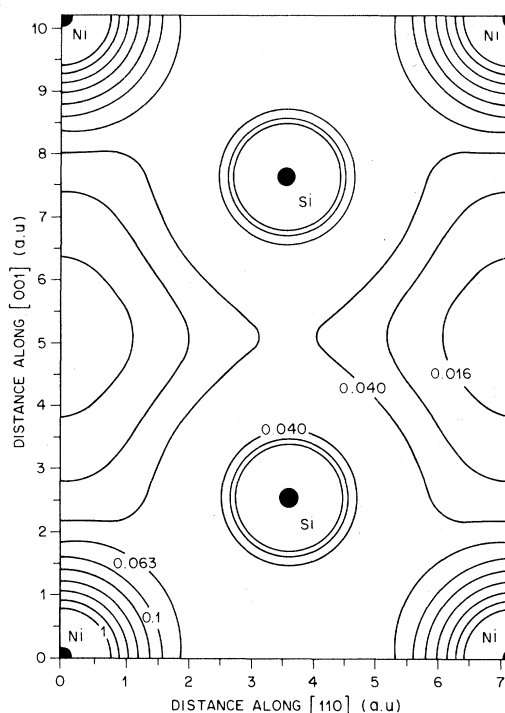


FIG. 5. Superimposed neutral atomic charge densities for NiSi_2 . Caption as in Fig. 4.

ple bonding-antibonding dichotomy is replaced by a much more complex set of possibilities with, presumably, a distribution of energies. The valence bands of Si, formed entirely from bonding sp^3 pairs, have a highly structured density of states with three prominent peaks which are absent in NiSi_2 . This structure has been related to wavefunction quantization conditions around the six-membered rings which make up the diamond structure.²¹ To draw the best parallel to this effect in NiSi_2 we consider two Si sp^3 hybrids which overlap through a common Ni as one link in possible ring structures. In terms of these links NiSi_2 has 2-, 3- and 4-member rings around a basic structural unit so several types of such quantization conditions exist. Both of the above effects combine to average out the Si sp^3 -related density of states to its simple-metal form, while maintaining a decidedly non-simple-metal-like charge distribution.

¹K. T. N. Tu and J. W. Mayer in *Thin Films—Interdiffusion and Reactions*, edited by J. M. Poate, K. N. Tu, and J. W. Mayer (Wiley, New York, 1978), p. 359.

²G. Ottaviani, *J. Vac. Sci. Technol.* **16**, 1112 (1979).

³P. S. Ho, G. W. Rubloff, J. E. Lewis, V. L. Moruzzi, and A. R. Williams, *Phys. Rev. B* **22**, 4784 (1980).

⁴J. H. Weaver, V. L. Moruzzi, and F. A. Schmidt, *Phys.*

- Rev. B 23, 2916 (1981).
- ⁵G. Ottaviani, K. N. Tu, and J. W. Mayer, Phys. Rev. Lett. 44, 284 (1980).
- ⁶J. L. Freeouf, G. W. Rubloff, P. S. Ho, and T. S. Kuan, Phys. Rev. Lett. 43, 1836 (1979).
- ⁷I. Abbati, L. Braicovich, B. DeMichelis, O. Bisi, C. Calandra, U. del Pennino, and S. Valeri, J. Phys. Soc. Jpn. 49, Suppl. A, 1071 (1980).
- ⁸P. T. Grunthaner, F. J. Grunthaner, and J. W. Mayer, J. Vac. Sci. Technol. 17, 924 (1980).
- ⁹P. S. Ho, P. E. Schmid, and H. Föll, Phys. Rev. Lett. 46, 782 (1981).
- ¹⁰K. C. R. Chiu, J. M. Poate, L. C. Feldman, and C. J. Doherty, Appl. Phys. Lett. 36, 544 (1980).
- ¹¹K. C. R. Chiu, J. M. Poate, J. E. Rowe, T. T. Cheng, and A. G. Cullis, Appl. Phys. Lett. 38, 988 (1981).
- ¹²The effect of low-energy preferential sputtering is being considered in another paper: Y. J. Chabal, A. Franciosi, J. H. Weaver, J. E. Rowe, and J. M. Poate, Phys. Rev. B (in press).
- ¹³D. R. Hamann, Phys. Rev. Lett. 42, 662 (1979).
- ¹⁴E. Wigner, Phys. Rev. 46, 1002 (1934), and also see Ref. 13.
- ¹⁵A. Baldereschi, Phys. Rev. B 7, 5212 (1973); D. J. Chadi and M. L. Cohen, *ibid.* 8, 5747 (1973); H. J. Monkhorst and J. D. Pack, *ibid.* 13, 5166 (1976).
- ¹⁶R. W. G. Wyckoff, *Crystal Structures*, 2nd ed. (Wiley, New York, 1973), Vol. 1, p. 242.
- ¹⁷V. L. Moruzzi, J. F. Janak, and A. R. Williams in *Calculated Electronic Properties of Metals* (Pergamon, New York, 1978).
- ¹⁸J. E. Rowe and N. V. Smith, Phys. Rev. B 10, 3207 (1974).
- ¹⁹O. Bisi and C. Calandra, J. Phys. C (in press).
- ²⁰J. van Vechten, Phys. Rev. 187, 1007 (1969).
- ²¹J. D. Joannopoulos and M. L. Cohen, Phys. Rev. B 7, 2644 (1973).